Journal of Conventional Weapons Destruction

Volume 18
Issue 1 *The Journal of ERW and Mine Action*

Article 16

April 2014

A Discrimination Method for Landmines and Metal Fragments Using Metal Detectors

Alex M. Kaneko
Tokyo Institute of Technology

Edwardo Fukushima
Tokyo Institute of Technology

Gen Endo
Tokyo Institute of Technology

A Discrimination Method for Landmines and Metal Fragments Using Metal Detectors

While discrimination methods for distinguishing between real mines and metal fragments would greatly increase the efficiency of demining operations, no practical solution has been implemented yet. A potentially efficient method for the discrimination of metallic targets using metal detectors uses a high-precision robotic manipulator to scan the minefield. Further field research is needed, however, before this method can deploy for operational use.

by Alex M. Kaneko, Edwardo F. Fukushima and Gen Endo [Tokyo Institute of Technology]

Current detection and clearance methods suffer from high false-alarm rates (FAR) and are costly, dangerous and time consuming. In 2001, the Tokyo Institute of Technology began work on a semi-autonomous mobile robot, the Gryphon (Figure 1), to facilitate the mine-detection process.[1] The robot's manipulator is equipped with tools for cutting vegetation and uses mine sensors to scan rough terrain, record data and note suspect locations by marking the ground. During experiments in test fields of flat terrain with no vegetation, the Gryphon proved as efficient as human operators when using a mine detector based on electromagnetic induction, such as a metal mine detector (MMD).[2] The Gryphon proved superior when compared to human operators in terms of reducing FAR and increasing probability of detection. However, similar to other demining solutions, FAR is still problematic with the Gryphon.

Problem Statement

One of the greatest problems in manual humanitarian landmine detection and removal involves high FAR, which are inherent to the use of electromagnetic induction-based detectors. Currently, no commercially available MMDs can distinguish landmines from other metal fragments. Some electromagnetic induction-based detectors, however, can select metal types to be searched, such as gold detectors.[3] Similarly, MMDs can be used for the discrimination of landmines and other metal fragments, as shown by research in the following topics:

1. Algorithms for evaluation of detected signals using models of physical phenomena[4,5,6]
2. Feature extraction from MMD signals and classification of data according to metal type, size or depth of the metal fragments[7,8,9]
3. Algorithms that combine time domain analysis and frequency domain analysis[10,11]

Some methods also rely on a dual-sensor approach, which combines two sensors and an MMD with ground-penetrating radar (GPR).[12,13] However, a high level of expertise is still needed to properly evaluate the obtained data (image or sound). Moreover, discrimination has a large safety margin, which keeps FAR high. Another interesting method that has been reported uses image processing, MMD-signal surface area and volume calculation to estimate size and material, followed by depth estimation, which is achieved by placing the MMD at different angles.[9] Despite reducing FAR to 39%, this method requires too much additional information from several depths (layers) besides the standard scan for discrimination, which considerably slows the demining operation by many minutes.[8]

Unfortunately, these methods have yet to be successfully implemented for use in practical demining tasks. Here, preliminary research on a potentially faster, newer, more accurate, on-site method (no need for additional scans) for discrimination of metallic targets using metal detectors is presented, and takes advantage of high-precision scans of the minefield using a robotic manipulator as shown in Figure 1.

Robotic Scanning and Sensor Data

The usual scanning procedure consists of manually swinging the MMD sideways while advancing the search head in increments between one scan and another. A robotic arm, which achieves higher precision and repeatability, can conduct a similar procedure. For a human deminer, the MMD signals (called V[%] here) are transformed into sound, and the deminer must remember and search the position of the ground target. For a robotic system, the sensor signal can be transmitted to a

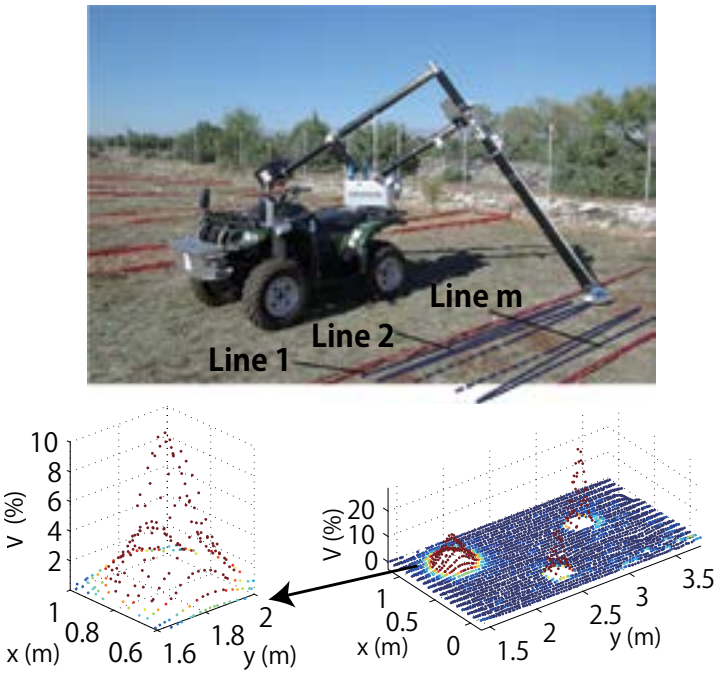

Figure 1. The demining robot Gryphon and its metal mine-detector signal visualization.
All figures courtesy of the authors.

computer and easily associated with the location of the manipulator. The signal can be processed in real time, and the user can easily visualize it (Figure 1). For the Gryphon system, the target position can be marked directly on the ground by painting or placing colored markers on the spot.[14]

SRMMDS uniqueness. Figure 2 shows a 3-D plot of the MMD signal, also known as a spatially represented metal mine-detector signal (SRMMDS). SRMMDS drastically changes according to postures and target types. Depending on the target, SRMMDS will present different characteristics, which can include physical properties such as depth, material, posture, shape, size and soil conditions. This implies that if a database of SRMMDS for every target in every condition could be prebuilt, one would only need to compare the SRMMDS obtained in the minefield to get the closest match in the database, which would identify the target, as well as the target's depth and posture. Even though some metal detectors can discriminate metal types, this feature is explored differently in this research.[3] Different metal types generate positive or negative SRMMDS, suggesting the type of metal. However, the combined characteristics that compose the detected SRMMDS are fundamental for identification in this research, features such as the depth, material, posture, shape, size and soil conditions. Although previous works used databases, this research has a different approach in which a high-precision robotic arm obtains SRMMDS. Simplified, only the necessary parts of the whole SRMMDS are stored in the database using simple yet powerful mathematical relations.[7,8]

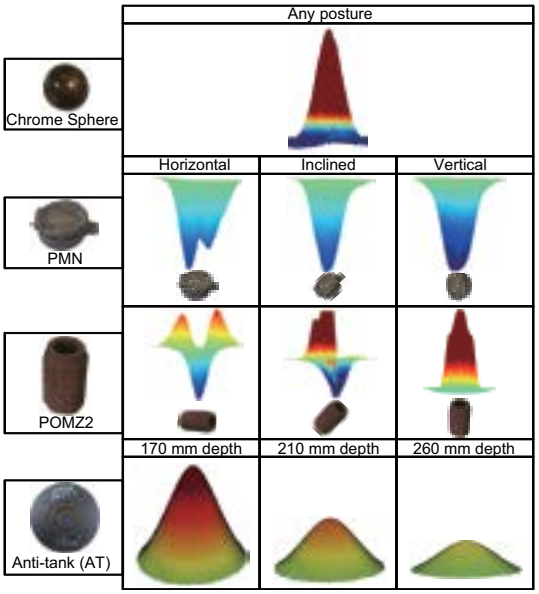

Figure 2. SRMMDS for different targets at different postures and depths.

SRMMDS simplification. In Figure 3, θ is defined as x'y'z', the local coordinate for SRMMDS. While the x'y' plane parallels the MMD scanning plane, the z'-axis passes through the maximum absolute point of the SRMMDS. The plane Pθ is orthogonal to the x'y' plane and passes through the z'-axis at an angle θ relative to the x'-axis. The intersection of plane Pθ and the SRMMDS contour generates a new curve, which is a characteristic curve known as V(r(θ)) (Figure 3) that is referenced to the new axis r(θ) and defined by the intersection of planes Pθ and x'y'.

Figure 3 demonstrates that the characteristic curves of physically symmetric targets such as anti-tank (AT) mines are the same for any angle θ, while curves for nonsymmetric targets change drastically. This analysis suggests that SRMMDS can be simplified to a set with a minimum number of characteristic curves. For symmetric cases, one characteristic curve would be enough, but this is not obvious for nonsymmetric cases. For the nonsymmetric targets (shown in Figure 2), a characteristic curve for the target's longest length of direction presents many inflections and peaks when compared to other angles. This research defines the characteristic curve with most inflections and peaks as the **main characteristic curve** and its axis r(θ) as the **main axis**. Figure 4 shows some examples of main characteristic curves.

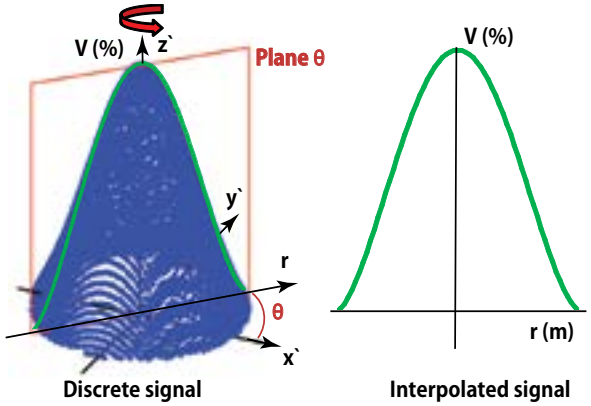

Figure 3. Cutting plane using as example the obtained signal of an anti-tank mine.

Polynomial Characterization

Characteristic curves can be represented by splines, polynomials or other mathematical relations in the form of V = f(r(θ)). As the number of inflections for the characteristic curves is limited, the authors propose polynomials in the form of Equation 1. This method has the advantage of keeping the signal characteristics and filtering part of the noisy raw data at the same time. In this work, all signals are translated with maximum peak in r = 0, making a_0 the maximum absolute MMD value of the signal.

Equation 1: $f(Y) = a_0 r(\theta)^0 + a_1 r(\theta)^1 + a_2 r(\theta)^2 + \ldots + a_n r(\theta)^n$
Where a_0, a_1, a_2,..., a^n are polynomial coefficients

In this research, the integral of the polynomials' difference (Equation 2) is adopted as the measure of error (*Err* [%])—i.e., similarity—between characteristic curves, which will serve as the main criteria for discrimination.

Equation 2: $Err = \int|f - g|/h*100$
Where *f* and *g* are polynomials to be compared
$h = max[\int|f|, \int|g|]$

Basic Discrimination Scheme

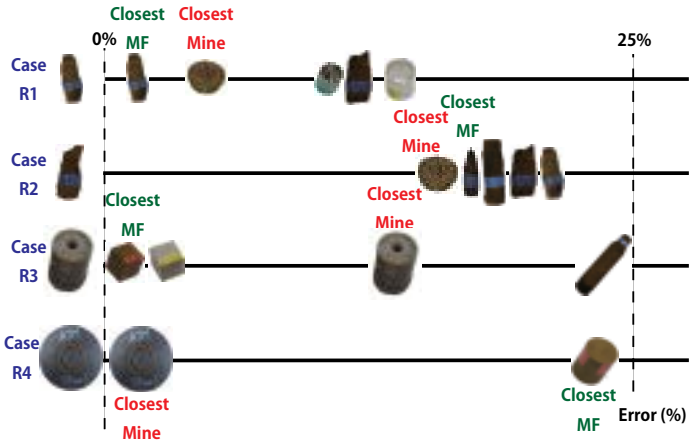

Figure 4. Examples of main characteristic curves with different peaks, intensities and sizes.

The basic scheme for discrimination of sensed signals can be implemented as follows:

- **Step 1**: Calculate the *Err* (Equation 2) for the characteristic curve of the sensed signal against all data in the prebuilt database.
- **Step 2**: Select the data with minimum *Err* as candidate for discrimination.

This scheme can result in four possible cases, namely R1, R2, R3 or R4, as shown in Table 1(a) and illustrated in Figure 5. Cases R1 and R4 result in correct discrimination. Although R2 results in a false positive and thus increases FAR, it is still acceptable. However, case R3 finds metal fragment data as the closest match for a landmine-obtained signal, causing a false negative result (mine judged as a metal fragment), which is unacceptable in this or any other demining research.

In this research, a false negative can be overcome by flagging as potential mines all metal fragment data that can cause case R3, resulting in a new case R3', as shown in Table 1(b). The identification of R3 and the R3' flagging are conducted during the database building and conditioning process, as explained in the database section.

Practical Discrimination Process

Measure of difference of errors (*dE*). In Figure 5, the *Err* of some metal fragment data is close to mines, as in the R1 example. To prevent any misjudgments in a real situation, Equation 3 calculates a measure of difference of errors (*dE*), which is the difference between the *Err* of the closest metal fragment ($Err_{(closest\ MF)}$) and the *Err* of the closest landmine ($Err_{(closest\ landmine)}$).

Equation 3: $dE = Err_{(closest\ MF)} - Err_{(closest\ landmine)}$

A threshold for *dE*, $dE_{threshold}$, is also defined for flagging all metal fragments in which $|dE| < dE_{threshold}$ as potential mines, thereby reducing the chance that landmines are discriminated as metal fragments.

Measure of confidence ($E_{threshold}$). Another case that can be observed in Figure 5 involves the *Err* of the closest target (called $E_{closest}$) that sometimes can be too high, which indicates no matches in the database. This can mean that the data contains too much noise or the target is degraded, making it a potential risk. In this research, a safety criterion labels the test subject as a potential mine when $E_{closest}$ is greater than a given threshold, $E_{threshold}$, to be determined by experiments. Figure 6 shows some examples of metal fragments similar to landmines.

Discrimination steps. The final scheme for discriminating sensed signals, while taking into account the above measures, is implemented as follows:

- **Step 1:** Calculate the *Err* of the obtained signal (sensed signal) against all available data in the database.
- **Step 2:** Select the data with minimum *Err,* i.e., $E_{closest}$.
  - » If Eclosest ≥ Ethreshold, consider the sensed signal as a potential mine and end discrimination.
- **Step 3:** Calculate the measure of difference of errors (*dE*), and make the final decision.
  - » If $dE > 0$, the sensed signal is considered a mine. If $dE < 0$ and $|dE| > dE_{threshold}$, the sensed signal is considered a metal fragment. Otherwise, the sensed signal is considered a potential mine.

Database-building Experiment

In order to verify the proposed method's validity, a database of characteristic curves (represented by polynomials) was built for multiple targets, depths and postures using a robotic manipulator. The data was taken with a metal mine-detector head at a linear speed of 50 mm/s, with a 10-mm depth step, 10-mm line step between scan lines and a signal output density of 0.2 points/mm. For the following analysis, data with weak signals ($V(\%) < 1\%$) and saturated signals ($V(\%) = 100\%$) were removed from the database.

a.

Case	Test Subject	Closest Match	Discrimination Result	
R1	Metal fragment	Metal fragment	True negative	Good: decrease FAR
R2	Metal fragment	Mine	False positive	Still acceptable: increase FAR
R3	Mine	Metal fragment	False negative	Not acceptable: a missed mine
R4	Mine	Mine	True positive	Good: increase probability of detection

b.

R3'	Mine	Potential mine	True positive	Good: increase probability of detection

Table 1.a and b. Basic discrimination cases according to *Err* (%). b. After the database conditioning process, case R3 becomes R3'.
Table courtesy of authors/CISR.

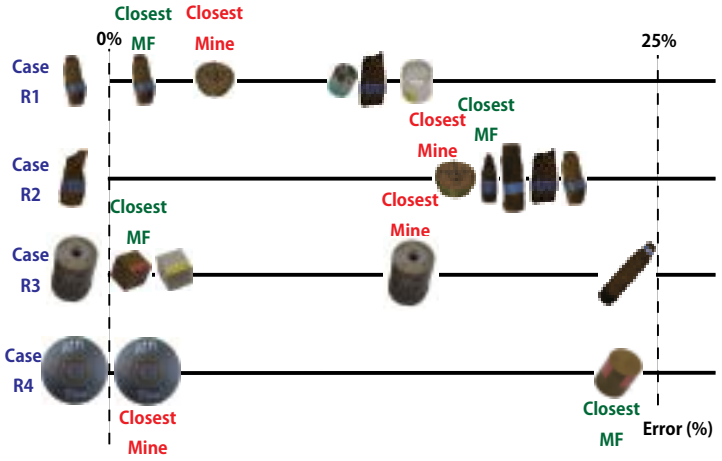

Figure 5. Basic discrimination cases (R1, R2, R3, R4) and target distances according to *Err*.

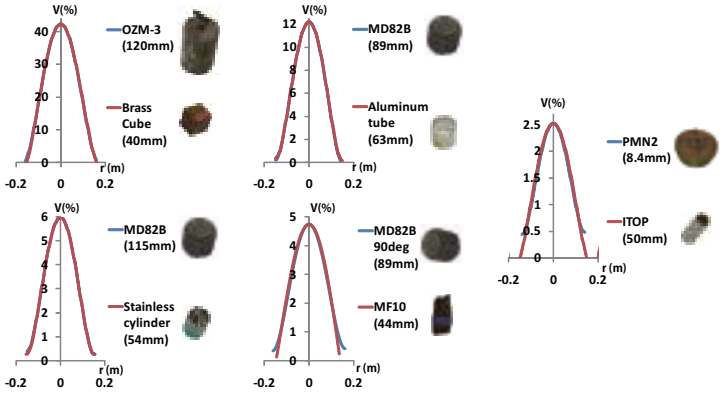

Figure 6. Examples of metal fragments considered potential mines by the $E_{closest}$ and $|dE| < dE_{threshold}$ criteria. Targets and corresponding depths are shown in parenthesis. Note that the International Test Operations Procedures (ITOP) conceived for an ITOP project as the metal content of larger stimulant mines shows SRMMDS very similar to the PMN2 mine and it is also classified as a potential mine by this criteria.

Metal detector signal conditioning. The Minelab F3 Metal Mine Detector was chosen for this experiment.[15] This detector outputs signals in two independent channels (called $\mathbf{Ch_A}$ and $\mathbf{Ch_B}$ here), which are combined according to Equation 4 and detailed in endnote 16.[16] $\mathbf{Ch_C}$ is used to derive characteristic curve $V(r(\theta))$ for comparison in Equation 2.

Equation 4: $Ch_C = Ch_B - Ch_A - median\ (Ch_B - Ch_A)$ (4)

Targets description. Figure 7 and Table 3 (page 62) show target types and testing conditions. A total of 42 different targets (11 landmines and 31 metal fragments) consisting of different shapes (cubes, cylinders, spheres, tubes) and materials (aluminum, brass, chrome, stainless, steel), with depths varying from 10 mm to 400 mm, and different

postures (horizontal, inclined 45˚ and vertical) were tested, which resulted in a total of 362 different data entries into the database. To be more applicable in an operational setting, future research efforts will increase the data library to include a range of minimum metal mines and small minefield fragments.

Database integrity and measure of confidence setting. For each given data *N* in the database (Table 3, *N* = 1 to 362), consider *N* as a test subject and calculate the *Err* (Equation 2) against all other data in the database. The cases (R1, R2, R3 and R4) described earlier are analyzed and shown (sorted for easier visualization) in Figure 8.

To determine $E_{threshold}$, several values from 0 to 100% were set, and corresponding values for false positives and true positives were observed. As Figure 9 (page 63) shows, $E_{threshold} = 10\%$ is the value that maximizes the difference between true positives and false positives.

Expanding Database Capabilities: Data Interpolation for Different Depths

Case	Type of Test Subject	Type of Closest Match	*dE*	Discrimination
R1	Metal fragment	Metal fragment	$dE < 0$, $\|dE\| > dE_{threshold}$	True negative
R1'	Metal fragment	Metal fragment flagged as "potential mine"	$dE < 0$, $\|dE\| \leq dE_{threshold}$	False positive
R2	Metal fragment	Mine	$dE > 0$	False positive
R3'	Mine	Metal fragment flagged as "potential mine"	$dE < 0$	True positive
R4	Mine	Mine	$dE > 0$	True positive

Table 2. Discrimination cases: For all the above cases when $E_{closest} \geq E_{threshold}$, test subject shall be considered a potential mine. *Table courtesy of authors/CISR.*

	Data Number	Target Type	Dimensions	Main Composing Material	Posture
Not landmines	1-186	Bullets and cartridges (MF01-MF21)	1-27mm diameter, 27-114 mm height	Steel	Horizontal
	187-222	Bullets and cartridges (MF01, MF19, MF21)	7-27 mm diameter, 27-114 mm height	Steel	45° in xz
	223-254	Cube	20 mm edge	Aluminum, stainless, brass	Horizontal
	255-274	Cylinder	11 mm diameter, 12.5 mm height	Aluminum, stainless, brass	Horizontal
	275-291	Tube	11-mm external diameter, 0.5 mm thickness, 12.5 mm height	Aluminum, stainless, brass	Horizontal
	292-301	Sphere	25.4 mm diameter	Chrome	Horizontal
	302-305	ITOP	4.8 mm outer diameter, 0.5 mm thickness, 12.5 mm height	Aluminum	Horizontal
Landmines	306-330	AT	300 mm diameter	Steel	Horizontal
	331-335	PMN	112 mm diameter 56 mm height	Mixture of small alloys	Horizontal
	336-340	PMN2	125 mm diameter 65 mm height	Steel	Horizontal
	341-362	Other landmines (p-40, PSM-1,MD82B, etc.)	Many variations	Steel	Many variations (horizontal, vertical and 45° in xz)

Table 3. Dimensions of the targets used for building the database. *Table courtesy of authors/CISR.*

Preparing a database containing information for every depth and posture may be infeasible in reality. Fortunately, a given target's characteristic curves basically keep the same level of concavity and mainly change in amplitude (a_0) for different depths, as Figure 10 (page 63) shows. For each value of r(m), MMD signals for the main characteristic curves of each depth have a quadratic relation. For example, if the input a_0 is 80%, the estimated depth is around 160 mm for the AT mine and 80 mm for metal fragment 21. This strong relation between depth and signal intensities suggests that we can estimate characteristic curves from a desired depth or vice versa by interpolation (represented in red). In this work, a_0 is used as input for interpolation, which generates a depth and a main characteristic curve for each target and is used for comparison in Equation 2. The data with $E_{closest}$ is then output, providing suggestions for depth, material, posture and target type.[17]

Repeating the analysis necessary to measure confidence setting with the interpolation method, smaller values of *Err* are obtained. In the new threshold, $E_{threshold}$ equals 15% (Figure 11, page 63), and R1, R2, R3 and R4 cases are set. Since no extrapolation is done in the interpolation, part of the data (each target's deepest and shallowest data) is not used. Since depth errors are possible, depth-error margins are also considered; Figure 12 (page 63)shows the analyzed trade-off.[17] For interpolated cases, FAR levels are much lower when compared to the Discrete Data 10 mm case.

Figure 12 shows a FAR analysis conducted in a laboratory with the data from the database. Since potential mines were flagged with the cri-

Figure 7. Targets used for building the database.

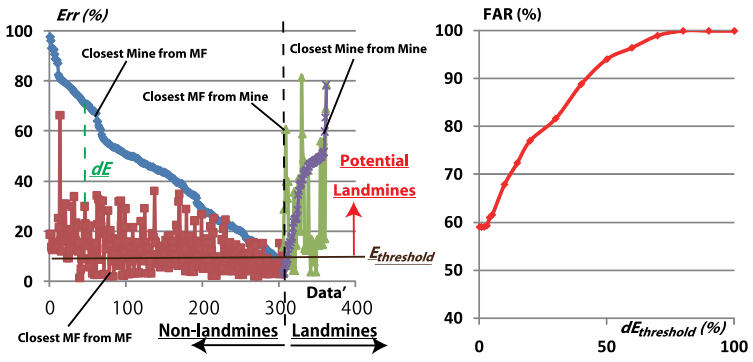

Figure 8. Resulting errors of closest metal fragments and mines from each data. According to the adopted safety margins $dE_{threshold}$ and $E_{threshold}$ different FAR can be observed.

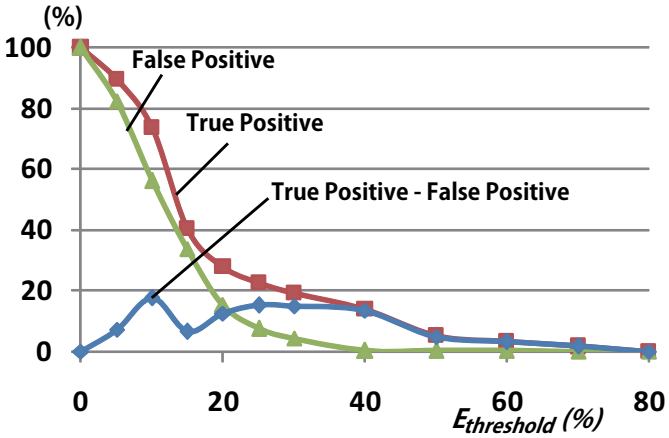

Figure 9. Variation of false-positive and true-positive values according to $E_{threshold}$ (discrete case).

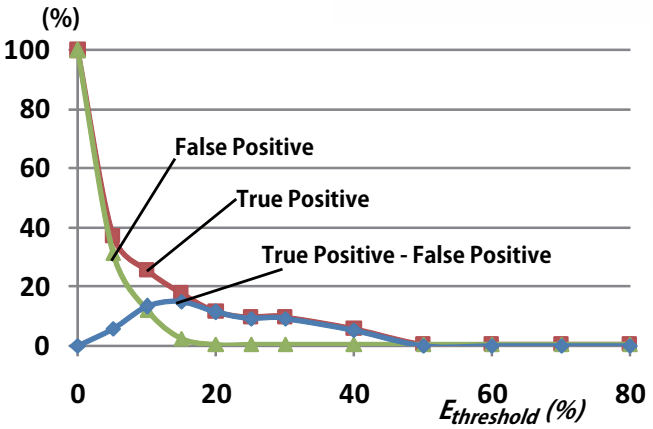

Figure 11. Variation of false-positive and true-positive values according to $E_{threshold}$ (interpolated case).

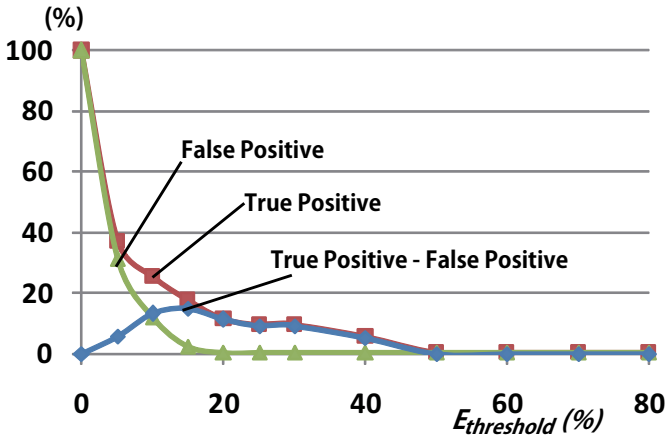

Figure 10. Example of polynomial interpolation for an AT target type MF21 target type. Strong relation between depths and MMD signals permit main characteristic-curves estimation by interpolating the available data in the database.

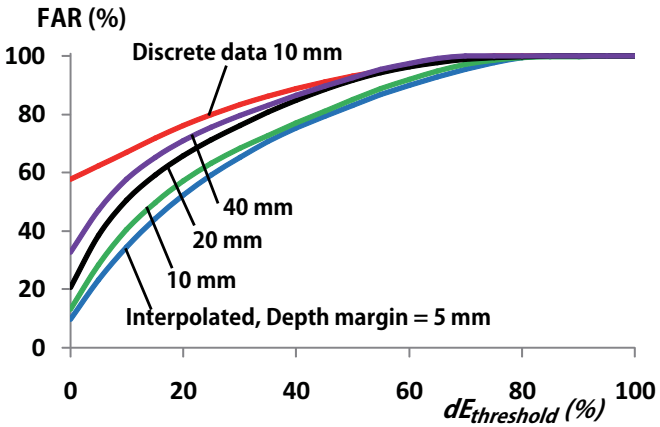

Figure 12. Trade-off of adopted safety margins and FAR. For all cases, FAR is generated with no occurrence of false negatives due to the discrimination criteria and safety margins adopted.

teria shown in the above section on discrimination, Figure 12 shows all cases in which false negatives do not occur, even if $dE_{threshold} = 0$. However, in real demining operations, $dE_{threshold} = 0$ is unacceptable, and a convenient safety margin must be set. In Figure 6 (page 61), an International Test Operation Procedures (ITOP) target resembles a PMN2 mine, and it is considered a potential mine in the discrete case in which $|dE| < dE_{threshold}$ criterion when $dE_{threshold} \geq 10\%$. Therefore, $dE_{threshold} = 10\%$ is adopted. For interpolated cases, Equation 2 identifies an ITOP target as a potential mine. While $dE_{threshold} = 0$ would be enough, a minimum of $dE_{threshold} = 5\%$ is adopted. Moreover, since the maximum depth-estimation error of this method is 40 mm, this depth margin is adopted in real operations.[17]

Experimental Results

In this section, data taken in 2007 is used at a test field in Croatia.[2] The Gryphon robot conducted this test. The test scanned uneven lanes of different soil properties, where several metal fragments and ITOP containing landmine surrogates were buried in random positions at depths between 1 and 14.5 cm. Among the six lanes and 38 targets per lane (180 data points in total, of which 120 were ITOP), 14 ITOP containing landmine surrogates and 14 metal fragments (bullets, rockets, etc.) were chosen to be applied as input in the proposed discrimination method. The data was chosen so that no other metal fragments were nearby, and the position was located within a standard scan area (2 sq m) to avoid cutting data. Table 4 (page 64) shows the safety margins and results.

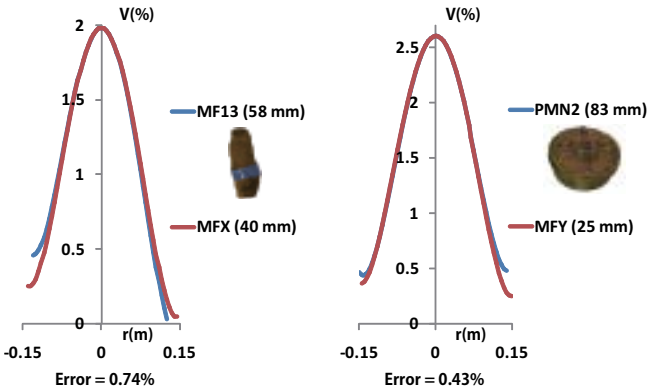

Figure 13. FAR examples: Fragment discriminated as potential mine (left) and fragment discriminated as landmine (right). Each target's depth is shown in parenthesis. MFX and MFY are two metal fragments from the test field, of which size, shape and material are unavailable.

The adopted safety margins guarantee correct detection of all ITOP targets as potential mines. In the laboratory, all ITOP data (in discrete and interpolated cases) are the closest targets to metal fragment 10 (cartridge shown in Figure 7 and Table 3, page 62). In this experiment with ITOP data from the test field, six of the 14 instances for discrete cases and 12 of the 14 for interpolated cases designated metal fragment 10 as the

	Discrete	Interpolated
Ethreshold (%)	10	15
dEthreshold (%)	10	5
Depth margin (mm)	40	40
Metal fragments discriminated as "potential mines" according to Ethreshold criterion	8/14	5/14
Metal fragments discriminated as "potential mines" according to dEthreshold criterion	5/14	1/14
Metal fragments discriminated as landmines by closest data in database	0/14	1/14
FAR (%)	13/14 = 92%	7/14 = 50%
ITOPs discriminated as "potential mines" according to Ethreshold criterion	3/14	0/14
ITOPs discriminated as "potential mines" according to dEthreshold criterion	9/14	13/14
ITOPs discriminated as ITOP itself in vertical posture by closest data in database	1/14	1/14
Discriminated as landmine by closest data in database	1/14	0/14
False negatives	0/14	0/14
Time for discrimination/target (s)	< 1	< 1

Table 4. Parameters adopted and results of the proposed method.
Table courtesy of authors/CISR.

closest target using direct search with Equation 2, which was consistent in the laboratory environment. The ITOP in the upright position in the database (not buried in the laboratory environment) and the safety margin criteria are valid for correct discrimination of data obtained with the Gryphon in soil.

A large number of the metal fragments were discriminated as potential mines in the discrete case due to the $E_{threshold}$ criterion, which indicates no similar targets exist in the database. This experiment detected eight out of 14 instances for discrete cases and five out of 14 metal fragments for interpolated cases. Due to the method's adopted safety precautions, these results were expected. Adding similar target information to the database would result in more accurate discrimination.

Based on their proximity to some landmines, two of the 14 metal fragments were considered potential mines by $dE_{threshold}$ criterion. Without available information on the test field's metal fragment material, shape or size, they will be known as metal fragment X (MFX) and metal fragment Y (MFY). In interpolated cases, MFX was considered a potential mine for being too similar to the metal fragment 13 cartridge (Figure 7 and Table 3, page 62) and was also considered a potential mine for being too similar to the PMN2 landmine (Figure 13, page 63). MFY was identified as a landmine by direct search, in which a PMN2 was identified as the closest data match (Figure 13, page 63).

The better performance of the interpolated method generates lower FAR levels. Time is another great advantage of using this method; it takes one second per target, which is faster than the false-alarm reduction method endnote 9 references, which takes more than 96 seconds per target.[9]

Conclusions

The above tests of this new methodology for the discrimination of landmines and metal fragments using commercially available MMDs and a prebuilt library demonstrate that this methodology can lead to effective signal characterization and real-time discrimination. Moreover, the methodology to interpolate discrete data into the database according to its depth makes the evaluation of data in arbitrary depths possible. False positives, which increase FAR, depend on the adopted error-margin criteria. After extensive laboratory tests, thresholds of $E_{threshold}$ (%) = 15% and $dE_{threshold}$ (%) = 5% were selected, which reduces the FAR to about 50%.

Results from the data analysis obtained in a Croatian test field in 2007 showed the robustness, validity and potential of the proposed method for practical applications. This technology could also potentially help detect unexploded ordnance (UXO) as well. However, additional testing with real UXO and mines, especially low-metal mines, will be needed if that application is pursued. Further tests in real minefields are in development as the next step in this work. This includes tests scheduled for 2014 in Angola that will investigate more types of landmines and metal fragments, as well as other important factors such as soil and climate.

JSPS KAKENHI Grant Number 25303012 supported this work.

See endnotes page 67

Alex M. Kaneko received a Bachelor of Engineering in mechatronics engineering from the University of Sao Paulo and a Master of Engineering in mechanical and aerospace engineering from the Tokyo Institute of Technology, where he is a doctoral candidate. His research activities include development of demining robots.

Alex Masuo Kaneko
Ph.D. Candidate
Department of Mechanical and Aerospace Engineering
Graduate School of Science and Engineering
Tokyo Institute of Technology
2-12-1 Ookayama, Meguro-ku
Tokyo 152-8552 / Japan
Tel/Fax: +81 3 5734 2648
Email: junjyouna.amk@gmail.com

Edwardo F. Fukushima is an associate professor at the Department of Mechanical and Aerospace Engineering of the Tokyo Institute of Technology. His research activities include the development of demining robots, design of controllers for intelligent robots and development of new brushless motors and drives.

Edwardo F. Fukushima, Dr. Eng.
Associate Professor
Department of Mechanical and Aerospace Engineering
Graduate School of Science and Engineering
Tel/Fax: +81 3 5734 3175
Email: fukusima@mes.titech.ac.jp

Gen Endo is an assistant professor at the Department of Mechanical and Aerospace Engineering of the Tokyo Institute of Technology. His research interests include mechanical design and intelligent control of mobile robots, especially in legged robots, leg-wheel hybrid robots, assistive mobile robots, educational robots and demining robots.

Gen Endo, Dr. Eng.
Assistant Professor
Department of Mechanical and Aerospace Engineering
Graduate School of Science and Engineering
Tel/Fax: +81 3 5734 2774
Email: gendo@mes.titech.ac.jp

ENDNOTES

U.S. and Vietnam Sign MOU by Cunningham [from page 6]

1. In Vietnam, this war is called the American War.
2. "Vietnam, US sign agreement for clearing war-era ordnance." *Thanhnien News*. 17 December 2013. http://bit.ly/1l7TeVn.
3. "Vietnam." *Landmine and Cluster Munition Monitor*. Last modified 30 August 2013. http://bit.ly/MaS3oW.
4. "Vietnam." Mines Advisory Group. Last modified 30 August 30 2013. http://bit.ly/1eWpfbo.
5. "Vietnam: Life-threatening Landmine Scavenging on the Increase." *IRIN News*. 1 January 2014. http://bit.ly/1cFqM4T.

Outcome Monitoring in Humanitarian Mine Action by Nedergaard [from page 7]

1. Millard, A.S., and K.B. Harpviken. "Reassessing the Impact of Humanitarian Mine Action." *PRIO Report 1/2000*. 2000. Accessed 17 September 2013. http://tinyurl.com/ny2m8a6.
2. See for instance: "Mine Action Evaluation: Evaluation Report of DFID Mine Action Funding." *WYG International Limited*. May 2013.
3. For more information, please refer to http://tinyurl.com/kb22drt, and download DDG's impact-monitoring manual.
4. Refer to the humanitarian accountability partnership (HAP) of which DDG is a partner. Accessed 20 August 2013. http://tinyurl.com/c3wyyt.
5. For more discussion, see Simister, N. "Developing M&E Systems for Complex Organisations: A Methodology." *INTRAC M&E Paper 3*. October 2009. Accessed 20 August 2013. http://tinyurl.com/luwowk9.
6. Chambers, Robert. "The Power and Potential of Participatory Statistics." Presentation at the Institute of Development Studies, University of Sussex, Brighton. 22 April 2013.
7. An informal mine action M&E practitioners meeting was held in Copenhagen to facilitate more knowledge-sharing on data collection within the sector. The meeting took place 2-3 July 2013 and included the following participants: UNMAS, UNDP, UNOPS, GMAP, MAG, NPA, DCA, GICHD and DDG.
8. After this article was written, a Statement on Outcome Monitoring in Mine Action was developed as a joint effort within the sector. The statement sets principles and guiding indicators for outcome monitoring in mine action. HI, MAG, NPA, DCA and DDG all signed up to the principles in the statement. Accessed 21 February 2014. http://bit.ly/1l5lcRm.

Amendments to the IMAS Land Release Series by Gray [from page 11]

1. The updated versions (07.11 Land Release, 0810 Non-technical Survey and 08.20 Technical Survey) are available to download at http://bit.ly/LPNUWP.

Effects of Mixed Teams on Land Release by Bini, Janssen and Jones [from page 14]

1. Baseline assessments were conducted in Afghanistan, Democratic Republic of the Congo, Iraq, Lebanon, Libya and South Sudan (two different organizations). These assessments were conducted for different organizations and have not been published.
2. Note that all answers from respondents represent their personal views and experiences and do not always reflect GMAP's views.
3. The land release process encompasses the efficient application of survey and clearance and the subsequent handover of land.
4. "Cartagena Action Plan 2010–2014: Ending the Suffering Caused by Antipersonnel Mines." *Cartagena Summit on a Mine-Free World*, Action No. 15, 20 and 52. Cartagena de Indias, Colombia, 30 November–4 December 2009. http://bit.ly/19c4WaL.
5. "Vientiane Action Plan." *Convention on Cluster Munitions*, Action No. 14. Vientiane, Laos, 12 November 2010. http://bit.ly/ILYkFm.
6. United Nations Mine Action Service. *IMAS 07.11*: Land Release. Section 5. New York: UNMAS, 10 June 2009. http://bit.ly/1fd3F4t.
7. Gender and Mine Action Programme. "Gender-sensitive recruitment and training in mine action: Guidelines." Geneva: GMAP, 2013. http://bit.ly/1aOjvNU.

Scalable Technical Survey for Improved Land-release Rates by Bach [from page 17]

1. Subdivision is normally only applicable to mine survey.
2. The latter implies, as a minimum, considerable increase in the percentage coverage during grid clearance, but more often it implies full clearance over the entire area if patterns are not determined. TS should not be considered light clearance of areas with low densities of mines. The latter would imply some form of risk mitigation, which is not the purpose of TS and may also be a violation of the conventions.
3. This process is less applicable when searching for CMR and not applicable when searching for other ERW.

Managing Residual Clearance: Learning From Europe's Past by Paunila [from page 22]

1. Creighton, Michael, Atle Karlson and Mohammed Qasim. "Cluster Munition Remnant Survey in Laos." *The Journal of ERW and Mine Action* 17, no. 2 (Summer 2013) 12–6. http://bit.ly/1k7xbci.
2. GICHD. "Sourcebook on Socio-Economic Survey." Geneva: GICHD, December 2011. Accessed 4 February 2014. http://bit.ly/1gwJHAz.